

Realization of optical perfect shuffle with microoptical array element

Ping Xu, Haixuan Huang, Kai Wang, Shuangchen Ruan, Jing Yang, Lili Wan, Xiangxian Chen, and Jiayong Liu

College of Electronic Science and Technology, Shenzhen University, Shenzhen, Guangdong, 518060, China
xuping@szu.edu.cn
<http://www.szu.edu.cn>

Abstract: A new method to realize the optical perfect shuffle (PS) with a microoptical array element is presented in this paper. The whole process is simulated by computer, and parameters of the structure to fabricate the experimental component are given. The microoptical array element has been fabricated by introducing very large scale integration (VLSI), stepping photolithography and reactive ion etching (RIE), which can realize 8-channel PS transformation. Experiments, tests and analysis have been done using the array element. The experimental results show that the method proposed in this paper agrees well with theoretical expectation. This success of the experiment lays a good foundation for us to do further research on realization of optical switching and communication through cascade multilevel PS interconnection.

©2007 Optical Society of America

OCIS codes: (350.3950) Micro-optics; (050.1380) Binary optics; (200.4650) Optical interconnects; (060.4510) Optical communication.

References and links

1. G. Eichmann and Y. Li, "Compact optical generalized perfect shuffle," *Appl. Opt.* **26**, 1167-1169 (1987).
2. A. W. Lohmann, W. Stork, and G. Stucke, "Optical perfect shuffle," *Appl. Opt.* **25**, 1530-1531 (1986).
3. K. H. Brenner and A. Huang, "Optical implementation of the perfect shuffle interconnection," *Appl. Opt.* **27** (1988).
4. Y. L. Sheng, "Light effective 2-D optical perfect shuffle using Fresnel mirrors," *Appl. Opt.* **28**, 3290-3292 (1989).
5. Shaoping Bian, Kebin Xu, and Jing Hong, "Optical perfect shuffle using Wollaston prisms," *Appl. Opt.* **30**, 173-174 (1991).
6. G. E. Lohman and A. W. Lohmann, "Optical interconnection network utilizing diffraction gratings," *Opt. Eng.* **27**, 893-900 (1988).
7. C. W. Stirk, R. A. Athale, and M. W. Haney, "Folded perfect shuffle optical processor," *Appl. Opt.* **27**, 202-203 (1988).
8. K. Hui, Z. Jiangying, and Z. Yuanling, "The implementation of FPS interconnection network using 2-D grating," *Acta Optica Sinica (Chinese)* **13**, 564-567 (1993).
9. Y.-I. Zhan, H. Kang, and J. -y. Zhang, "Optical implementation of the folded perfect shuffle interconnection network using quadrant-encoded gratings," *Opt. Eng.* **32**, 1657-1661 (1993).
10. Z. Jin and G. Weiqi, "Optical perfect shuffle using CGH element," *Acta Optica Sinica (Chinese)* **11**, 477-480 (1991).
11. H. Kang, Y. Zhan, J. Zhang, X. Huang, and X. Zhu, "Optical perfect-shuffle network implementation by use of an ordinary imaging system and holographic gratings," *Appl. Opt.* **33**, 2988-2990 (1994).
12. K. Choi and B. Lee, "A single-stage reconfigurable 2-D optical perfect-shuffle network system using multiplexed phase Holograms," *IEEE Photon. Technol. Lett.* **17**, 687-689 (2005).
13. N. Davidson, A. A. Friesem, and E. Hasman, "Realization of perfect shuffle and inverse perfect shuffle transformations with holographic elements," *Appl. Opt.* **31**, 1810-1812 (1992).
14. H. Kobolla, J. Schmidt, E. Gluch, and J. Schwider, "Holographic perfect shuffle permutation element for a miniaturized switching network," *Appl. Opt.* **34**, 2844-2847 (1995).
15. J. Liu, C. Zhao, and R. T. Chen, "Implementation of Optical Perfect Shuffle with Substrate Guided-Wave Optical Interconnects," *IEEE Photon. Technol. Lett.* **9**, 946-948 (1997).
16. Y. Baiying, *Applied Physics Optics* (Engineering Industry Press, China, 1990).

17. P. Xu, et al., "Optical perfect shuffle interconnection using computer-generated blazed grating array," *Opt. Rev.* **2**, 362-365 (1995).
18. P. Xu, et al., "Deep Etch Binary Optics Element," *Acta Optica Sinica (Chinese)* **16**, 1796-1801 (1996).
19. P. Xu, et al., "The even device fabricated by the deep etched binary optics technology for the exposure system of the quasi-molecule laser," *Science in China (Series E)* **45**, 1-9(2002).
20. P. Xu, et al., "Fabrication errors analysis and simulation of binary optical element," *Acta Optica Sinica (Chinese)* **16**, 833-838 (1996).
21. P. Xu, et al., "Theoretical analysis and design of perfect shuffle implementation using micro-optical array element," *Proc. SPIE* **5636**, 334-340 (2005).
22. P. Xu, et al., "Research on experiments of perfect shuffle implementation using micro-optical array element," *Proc. SPIE* **5636**, 374-378 (2005).

1. Introduction

With the persistent development of information superhighway and the rising digital optical computers, free spatial optical interconnection is being given increasingly close attention. Thereinto, a perfect shuffle (PS) network can be used as a basic network to realize any form of optical interconnection. Therefore, the PS transformation has its academic significance and applied value, and has excited extreme interest.

Some scholars have proposed several optical approaches to realize the PS transformation, such as using lenses and a prism system [1-5], diffraction grating [6-9], holographic optical elements [10-14] and substrate guided-wave optical interconnects [15]. However, there are some difficulties when these reported findings are used to implement the PS transformation in the optical interconnection, such as their complicated devices and failure to be cascaded.

In this paper, a new type element is presented, which can implement a PS network of free spatial optical interconnection. It is a microoptical array element, consisting of a series of sub-blazed gratings with different spatial frequency. In this paper, the microoptics array element is designed and simulated by a computer and the designed parameters are given; The micro optical array element has been fabricated by introducing VLSI, stepping photolithography and RIE, which can realize 8-channel PS transformation. The performance of the element is tested. Compared with the results of computer simulation, experimental results reveal that, with only one array element, the PS transformation can be easily realized, avoiding the additional use of complex optical device or spatial filtering to realize signal division, interleaving and order reversing. Output signals are upright and its signal duty ratio can be adjusted arbitrarily. The element has high efficiency of light energy and low channel cross talk. By this approach, it is convenient to realize microminiaturization and multilevel interconnection, and it is very useful when it comes to realize arbitrary levels of optical interconnection.

2. Schemes of design

2.1 PS Transformation

PS transformation refers to an operation which divides a group of N inputs into two halves and then interlaces the inputs from one half into the others, as shown in Fig. 1. Suppose there are N inputs, according to certain request, an arbitrary permutation can be obtained by continuously performing the PS transformation for $3\log_2 N$ times on a group of N inputs. Therefore, the PS network can be used as a basic network for the optical computers and optical interconnection.

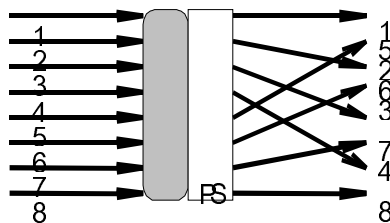


Fig. 1. PS transformation

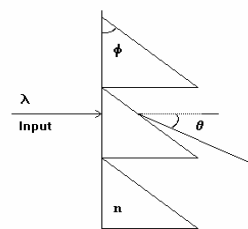


Fig. 2. Blazed grating

2.2 Principle of Blazed Grating

The Grooves and principle of blazed grating are shown in Fig. 2. When blazed angle ϕ satisfies the following equation [16]:

$$\phi = k\lambda / [(n-1)p] \quad (1)$$

The blazed grating will produce blazing output in θ direction:

$$\sin(\theta) = k\lambda / p \quad (2)$$

Where k is the blazing level (usually we let $k = 1$), λ is the blazed wavelength, p is the period of the blazed grating, and n is the index, as shown in Fig. 2. The blazed grating concentrates light energy to only one output level and its diffraction efficiency can theoretically reach 100%.

2.3 Schemes of the Design of the Microoptical PS plate

According to the rule of PS transformation and the principle of blazed grating, a PS plate can be designed and fabricated with the technology [17-20] we developed to fabricate microoptical elements. The main idea for design is as follows: Light can be output in different directions when it goes through gratings with different spatial frequencies. With gratings combined properly, a light beam is accurately controlled to output [20], abiding by the rules of the PS transformation. Therefore, an array element composed of micro-blazed gratings with different spatial frequencies is designed to realize the PS transformation. Due to the use of structure combined by deep relief blazed gratings, the element has a very high efficiency of light energy.

The PS plate we have designed is shown in Fig. 3 and a cross-sectional profile of its grooves is shown in Fig. 4. It consists of 8 blocks of sub-blazed grating, a total area of about $35 \times 22 \text{ mm}^2$. Along Y-direction it divides into 8 blocks. The 1st and 8th blocks are completely transparent, while the 2nd, 3rd, 4th are made up of blazed gratings with different spatial frequencies and blazed angles, whose grooves are parallel to Y-direction. Correspondingly, the 5th, 6th, 7th blocks are symmetrical to the 4th, 3rd and 2nd blocks, respectively. Therefore we can discuss the upper-half only.

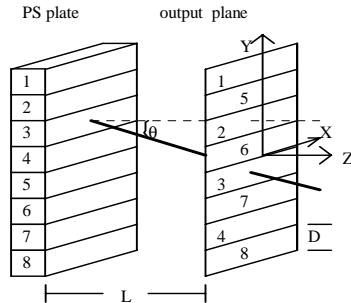


Fig. 3. Computer-generated PS plate

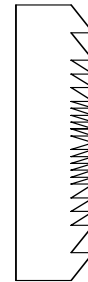


Fig. 4. Grooves of the PS plate

From the principle of blazed grating and transformation rule of PS plate, in fact, we know that to achieve PS transformation, we just need to choose a group of proper spacial frequencies respectively to the 2nd, 3rd and 4th sub-gratings.

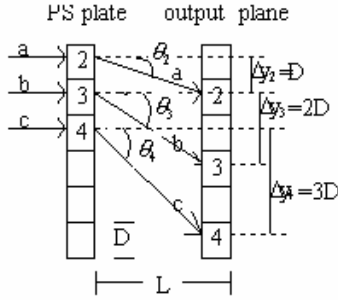


Fig. 5. Partial cross-sectional profile of the PS plate

For the sake of distinction we consider situations in which signals a, b and c pass through the 2nd, 3rd and 4th sub-gratings respectively. As shown in Fig. 5, these signals will have a different lateral displacement Δy_2 , Δy_3 and Δy_4 , respectively, along Y-direction in the output plane at a distance L apart from the PS plate. In order to achieve PS transformation these displacements must satisfy the following equation:

$$\Delta y_2 = D, \Delta y_3 = 2D, \Delta y_4 = 3D \quad (3)$$

Where D is the width of each sub-grating in Y-direction.

From geometrical relations in Fig. 5, we have the following equations:

$$L \cdot \tan(\theta_2) = D, L \cdot \tan(\theta_3) = 2D, L \cdot \tan(\theta_4) = 3D \quad (4)$$

Considering Eq. (2), Eq. (4) can be calculated as follows:

$$p_2 = (k\lambda / D)\sqrt{D^2 + L^2}, p_3 = (k\lambda / 2D)\sqrt{4D^2 + L^2}, p_4 = (k\lambda / 3D)\sqrt{9D^2 + L^2} \quad (5)$$

Where p_2 , p_3 and p_4 are periods of the 2nd, 3rd and 4th sub-gratings, respectively. That is to say, we can fabricate a PS plate whose designed parameters are chosen from Eq. (5) to realize the optical perfect shuffle.

3. Results of simulation by computer

Because of the computer's finite spatial bandwidth, it should be pointed out that satisfying Eq. (5) exactly is impossible in practical fabrication by computer. Therefore, the needs of design and fabrication must be weighed to choose proper parameters in practice. According to the experience mentioned above, we have chosen parameters as follows:

Table 1. Fabrication data of designed PS plate

Etched-phase depth	Wavelength λ (μm)	D (μm)	L (mm)	p_2 (μm)	p_3 (μm)	p_4 (μm)
4π	0.6328	4352	526	153	76.5	51

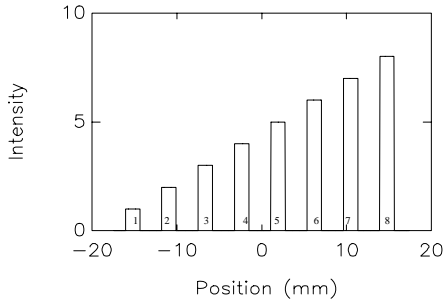


Fig. 6. Intensity distribution of input signal

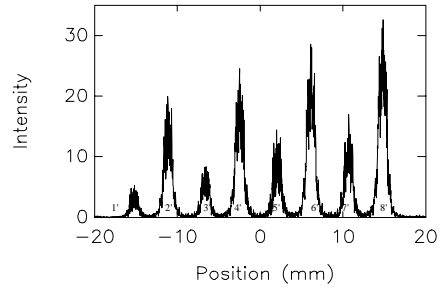


Fig. 7. Intensity distribution of output signal

Figure 6 is the intensity distribution of the input signal, and Fig. 7 is the output distribution on the output plane at a distance L apart after PS transformation. Table 2 shows standardized intensity data of input and output signals, which correspond to Figs. 6 and 7 respectively.

In Fig. 6 the order of position is $\{1, 2, 3, 4, 5, 6, 7, 8\}$, and in Fig. 7 it is $\{1', 2', 3', 4', 5', 6', 7', 8'\}$. Comparing the two figures, we learn that there are the following corresponding relationships between them: $1' \leftrightarrow 1, 2' \leftrightarrow 5, 3' \leftrightarrow 2, 4' \leftrightarrow 6, 5' \leftrightarrow 3, 6' \leftrightarrow 7, 7' \leftrightarrow 4, 8' \leftrightarrow 8$. Therefore, the order of position in Fig. 7 is actually $\{1, 5, 2, 6, 3, 7, 4, 8\}$. That is, after this transformation, the order of position has been changed from $\{1, 2, 3, 4, 5, 6, 7, 8\}$ to $\{1, 5, 2, 6, 3, 7, 4, 8\}$. Obviously, this change of position order arrangement exactly satisfies the PS transformation rule shown in Fig. 1.

Table 2. Standardized intensity distribution of the input and output signals

Position No.	1	2	3	4	5	6	7	8
Intensity of input signals	0.0278	0.0556	0.0833	0.1111	0.1389	0.1667	0.1944	0.2211
Homologue Position No.	1'	3'	5'	7'	2'	4'	6'	8'
Intensity of output signals	0.0262	0.0501	0.0742	0.0871	0.1090	0.1413	0.1700	0.1961
D.E (%)	94.24	90.11	89.08	78.40	78.47	84.77	87.49	88.69
Average Diffractive Efficiency (%):	86.41							

D.E: diffractive efficiency.

Now we give a brief discussion on the cross talk of the PS transformation. In Table 2, we calculate the diffractive efficiency (DE) as the intensity rate of output and input in each block. Considering the same designed empty-occupation of each input signal, the companion peak around each output signal, whose width is expanded to be a little larger than that of the input signal, is considered as the major part of the cross talk, reducing the DE, as shown in Fig. 7.

Table 3. Standardized intensity distribution of only one input signal

Position No.	1'	2'	3'	4'	5'	6'	7'	8'
D.E (%)	0.98	0.01	0.03	2.60	0.05	0.23	82.35	0.30

For reasons of distinction, we discuss the inter-influence among output signals. Considering only one signal, No. 4 passing through Block 4 while the other signals are sheltered from light, as shown in Fig. 8. Figure 9 and Table 3 show the standardized intensity distributions and data on output, respectively. According to Table 3, when only one channel

has been reserved and other channels have been sheltered, for instance when Channel 4 is reserved, 82.35 percent of the signal energy is output to Channel 7' and there is spatial expansion of the width of the output channel spot. Simultaneously, little optical energy is output to other channels (The most energy in which 7 other Channels has received reaches merely 2.6%). This phenomenon results in the cross talk among each channel. When all channels are unclosed, this cross talk is superposed among each channel and finally leads to the mixing of information. As can be seen from Table 2 and Table 3, most optical energy of each input signal is output to the corresponding output channel, and the optical energy which output to other non-expected channel accounts for very little bit. Therefore, we come to the conclusion that there is little inter-influence among output signals and the cross talk has little influence on the performance of the element.

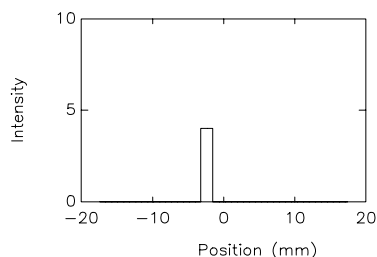


Fig. 8. Intensity distribution of one input signal

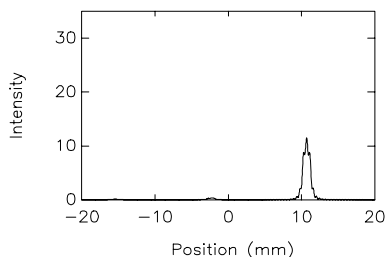


Fig. 9. Output intensity distribution of one input signal

By the way, there are two other causes for the occurrence of the cross talk. The first one is quantized errors, and the second is the values selected after optimization do not satisfy Eq. (5) exactly, due to the limitation of the image generator. These errors can be managed to an acceptable range.

In addition, in practical facture of the element, contraposition error on the etching depth is another cause for the occurrence of the cross talk.

4. Experimental setup and results

In our experiments, a He-Ne laser is served as light source. The laser beam is expanded and collimated before it turns into parallel light, and then it goes through a diaphragm and is applied to the 8-channel microoptical array element. The experimental setup is shown as Fig. 10. An optical power meter made by COHERENT Corporation in USA is used for detecting the laser power. (Its working spectrum ranges from 400nm to 1064nm, and the detecting power ranges from 10nW to 50mW)

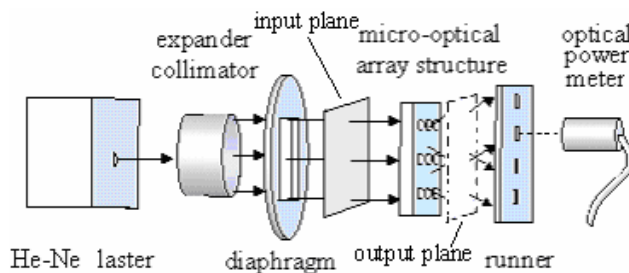


Fig. 10. The experimental setup of PS transformation

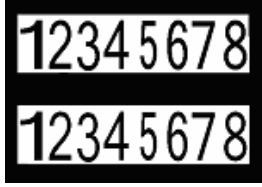


Fig. 11. The input signals



Fig. 12. The output signals

The input signals designed and fabricated for the experiment are shown in Fig. 11. Let the contents of the input signals be a set of integers $\{1, 2, 3, 4, 5, 6, 7, 8\}$, which arrange in two rows: the upper row and the nether row. Hereinto, the upper row is used for comparison instead of performing the transformation, and the nether row is the actual input signals. The input signals are applied to the PS plate, which consists of 8-channel micro optical array element. After the illumination of parallel light and the transformation performed by the element, the experimental result is displayed in Fig. 12. As shown in Fig. 12, the upper row is the projection of input signals that do not perform the transformation, and the nether row is the output signals after transformation.

The serial numbers of the input channels are $I_1, I_2, I_3, I_4, I_5, I_6, I_7, I_8$, and the corresponding sequence of the input signals is $\{1, 2, 3, 4, 5, 6, 7, 8\}$. The serial numbers of the output channels are $O_1, O_2, O_3, O_4, O_5, O_6, O_7, O_8$. What is apparently displayed in the nether row in Fig. 12 is that the sequence of the output signals is $\{1, 5, 2, 6, 3, 7, 4, 8\}$. That is to say after the transformation performed by the element the sequence of the input signals, which is $\{1, 2, 3, 4, 5, 6, 7, 8\}$, has been transformed into a sequence which is $\{1, 5, 2, 6, 3, 7, 4, 8\}$. Apparently, such a sequence transformation agrees well with the rule of perfect shuffle shown in Fig. 1.

Results from the experiment suggest that optical PS transformation can be successfully realized by using only one element.

5. Tests and analysis of the efficiency and cross talk

To test the efficiency and cross talk of each channel, a structure of runner is specially designed, as is shown in Fig. 13.

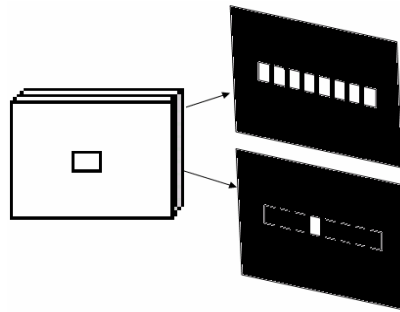


Fig. 13. Structure of the runner

With the devices shown in Fig. 10 and Fig. 13, only one channel has been reserved and other channels have been sheltered to measure the efficiency and cross talk of each channel. A screen with a rectangle aperture about a channel-width is attached to the 8-channel microoptical array element. As a result, the laser beam is limited to go through only one channel. An optical power meter is used to measure light power of the input channel. Next, the runner is dragged to measure respectively the light power of each output channel. The metrical result is shown in Table 4.

Table 4. The analysis of diffraction efficiency and crosstalk to each channel (Unit: %)

Output Input		O ₁	O ₂	O ₃	O ₄	O ₅	O ₆	O ₇	O ₈
		1	2	3	4	5	6	7	8
I ₁	1	95.30							
I ₂	2	1.42	6.59	78.57	1.89	0.50	0.47	1.47	0.36
I ₃	3	7.63	0.94	3.16	1.90	79.03	4.14	0.52	0.57
I ₄	4	3.21	0.44	0.65	0.90	0.68	2.38	88.95	1.09
I ₅	5	1.05	86.86	1.70	0.83	5.23	0.55	0.40	2.20
I ₆	6	0.67	1.61	2.08	73.86	2.94	3.99	0.64	7.61
I ₇	7	0.62	0.80	0.59	0.81	2.47	80.00	4.24	1.16
I ₈	8								94.05

Now we perform a brief analysis according to the data in Table 4.

First, the light power that output abiding the rule of perfect shuffle for each channel is relatively high. Taking the 4th input channel I₄ for example, the input power is mainly output in O₇, reaching 88.95%. The other channels can be analyzed similarly. It is concluded that the element has relatively high light utilization efficiency and its average transpositional efficiency reaches 84.58%, though a little lower than the efficiency worked out by the computer (86.41%).

Second, the power output to other channels is rather low; that is to say, the element has very low cross talk to other channels. The same conclusion comes out, based on the analysis of other input channels. Consequently, input signals have little influence on each other.

Of course, the diffractive efficiency obtained from the experiment is lower than our theoretical value. The main reasons may lie in the error during the fabrication of the element and the error in experimental tests, such as instability of the laser's output power, error of the optical path collimation, the observation error when we dragged the runner. These factors are to be improved further.

6. Conclusions

A new method to realize optical perfect shuffle with a micro optical array element is presented in this paper. The whole process is simulated by computer and results of the simulation confirm the feasibility of our designed scheme. Reliable parameters to fabricate the experimental component are given. The binary array element has been fabricated by introducing VLSI, stepping photolithography and RIE, which can realize 8-channel PS transformation. Experiments, tests and analysis have been done using the element. The result of experiments reveals that the PS transformation can be easily realized with only one array element, avoiding the additional use of complex optical device or spatial filtering to realize signal division, interleaving and order reversing, and the average efficiency reaches 84%. It can output erect image and has a high efficiency of light energy, accompanied by rather low cross talk. The experimental result indicates that the method proposed to realize the PS transformation by using micro optical array element [21-22] is feasible and agrees well with theoretical expectation. This success of the experiment lays a good foundation for us to do further research on the optical switching through cascade multilevel interconnection.

Acknowledgments

This work is supported by the National Nature Science Foundation of China (No.60178023) and the Science & Technology Development Foundation of Shenzhen. (No.200311).